

Longitudinal double-spin asymmetries in semi-inclusive deep-inelastic scattering of electrons and positrons by protons and deuterons

P.V. Kravchenko^{*†}

Petersburg Nuclear Physics Institute named by B.P.Konstantinov of National Research Centre "Kurchatov Institute (PNPI)", 188300 Gatchina, Russia

E-mail: kravchenko_pv@pnpi.nrcki.ru

A comprehensive collection of results on longitudinal double-spin asymmetries is presented for charged pions and kaons produced in semi-inclusive deep-inelastic scattering of electrons and positrons on the proton and deuteron, based on the full HERMES data set. The dependence of the asymmetries on hadron transverse momentum and azimuthal angle extends the sensitivity to the flavor structure of the nucleon beyond the distribution functions accessible in the collinear framework. No strong dependence on those variables is observed. In addition, the hadron charge-difference asymmetry is presented, which under certain model assumptions provides access to the helicity distributions of valence quarks.

*23rd International Spin Physics Symposium - SPIN2018 -
10-14 September, 2018
Ferrara, Italy*

^{*}Speaker.

[†]On behalf of the HERMES collaboration.

1. Introduction

Longitudinal double-spin asymmetries in polarized deep inelastic scattering (DIS) have since many years provided a window to study the spin structure of the nucleon by HERMES [1] and other experimental collaborations. Semi-inclusive DIS, in which an identified final-state hadron is observed in conjunction with the scattered lepton, have provided enhanced sensitivity through the fragmentation process to quark flavor and hence to individual parton distributions. A detailed theoretical picture has been developed, providing a framework for which semi-inclusive DIS measurements in any configuration of beam and target polarization are related to various combinations of distribution and fragmentation functions [2, 3]. If terms that depend on transverse nucleon polarization are neglected, the complete model-independent decomposition of the semi-inclusive DIS cross section in the one-photon-exchange approximation can be expressed in terms of moments of azimuthal modulations [3],

$$\frac{d\sigma^h}{dx dy dz dP_{h\perp}^2 d\phi} = \frac{2\pi\alpha^2}{xyQ^2} \frac{y^2}{2(1-\varepsilon)} \left(1 + \frac{\gamma^2}{2x}\right) \left\{ F_{UU,T}^h + \varepsilon F_{UU,L}^h + \lambda\Lambda\sqrt{1-\varepsilon^2} F_{LL}^h \right. \\ \left. + \sqrt{2\varepsilon} \left[\lambda\sqrt{1-\varepsilon} F_{LU}^{h,\sin\phi} + \Lambda\sqrt{1+\varepsilon} F_{UL}^{h,\sin\phi} \right] \sin\phi \right. \\ \left. + \sqrt{2\varepsilon} \left[\lambda\Lambda\sqrt{1-\varepsilon} F_{LL}^{h,\cos\phi} + \sqrt{1+\varepsilon} F_{UU}^{h,\cos\phi} \right] \cos\phi \right. \\ \left. + \Lambda\varepsilon F_{UL}^{h,\sin 2\phi} \sin 2\phi + \varepsilon F_{UU}^{h,\cos 2\phi} \cos 2\phi \right\}. \quad (1.1)$$

The angle ϕ is the azimuthal angle of the hadron momentum vector \mathbf{P}_h about the virtual-photon direction with respect to the lepton-scattering plane as depicted in Fig. 1 and defined, e.g., in Ref. [4]. The $F_{XY,Z}^{h,mod}$ of equation represent structure functions whose subscripts denote the polarization of the beam, of the target (with respect to the virtual-photon direction), and—if applicable—of the virtual photon. The superscript indicates the dependence on the hadron type and the azimuthal modulation parametrized. Each of these structure functions is a function of x , Q^2 , z , and $P_{h\perp}$, where z is the fraction of the virtual-photon energy carried by the observed final-state hadron (in the target rest frame), while $P_{h\perp}$ is the magnitude of the hadron momentum component transverse to the virtual-photon direction. The helicity of the nucleon in the center-of-mass system of the virtual photon and the nucleon is denoted as Λ , while λ represents the helicity of the beam lepton. Furthermore, the “photon polarization parameter” $\varepsilon = \frac{1-y-\frac{1}{4}\gamma^2 y^2}{1-y+\frac{1}{4}y^2(\gamma^2+2)}$ is the ratio of longitudinal-to-transverse photon flux, where $\gamma = Q/v$, and α is the fine-structure constant.

In order to probe the polarization-dependent structure of the nucleon with minimal experimental systematic uncertainties, spin asymmetries are typically measured instead of cross sections. Ideally, cross sections are compared in all combinations of 100% polarized beams (with respect to beam direction) and targets (with respect to virtual-photon direction) to form [5]

$$A_{LL}^h \equiv \frac{\sigma_{+-}^h - \sigma_{++}^h + \sigma_{-+}^h - \sigma_{--}^h}{\sigma_{+-}^h + \sigma_{++}^h + \sigma_{-+}^h + \sigma_{--}^h}. \quad (1.2)$$

Here, $\sigma_{\lambda\Lambda}^h$ denotes the cross section in a given configuration of equal and opposite beam and target helicities. In a typical experimental situation of incomplete polarizations of beam and target, the degrees of polarization of the beam and target must be divided out. In the limit of small hadron transverse momentum ($P_{h\perp} \ll zQ$), the various contributions to $A_{LL}^h(x, Q^2, z, P_{h\perp}, \phi)$ can be expressed in

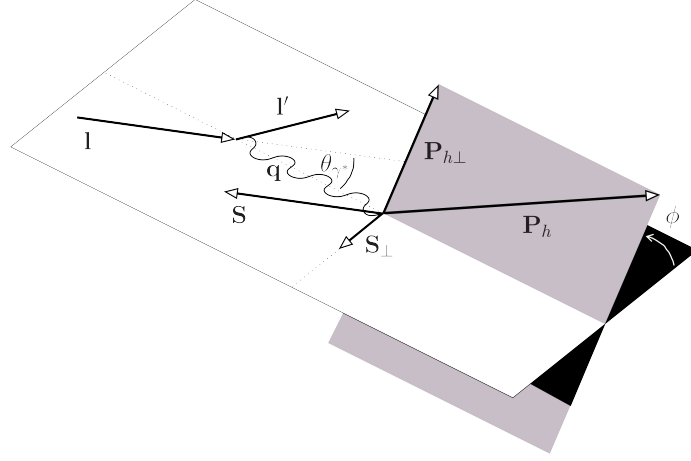


Figure 1: Following the *Trento conventions* [4], ϕ is defined to be the angle between the lepton scattering plane and the plane defined by the virtual-photon momentum $\mathbf{q} \equiv \mathbf{l}' - \mathbf{l}$ (the difference of the momenta of the outgoing and incoming lepton) and \mathbf{P}_h , the momentum vector of the observed hadron. \mathbf{S} is the spin vector of the nucleon (polarized along the direction of the incoming lepton), while \mathbf{S}_\perp is its component perpendicular to the virtual-photon direction.

terms of convolutions of TMD distribution with fragmentation functions. The azimuthally uniform $A_{LL}^h(x, Q^2, z, P_{h\perp})$ enters with a single leading-twist contribution:

$$F_{LL}^h \propto \sum_q e_q^2 \left[g_{1L}^q(x, p_T^2) \otimes_{\mathcal{W}_1} D_1^{q \rightarrow h}(z, k_T^2) \right]. \quad (1.3)$$

Here, “ $\otimes_{\mathcal{W}_1}$ ” represents a convolution of the distribution and fragmentation functions over the intrinsic transverse momentum p_T of the parton q (with fractional charge e_q) and the transverse-momentum contribution k_T from the fragmentation process with a kinematic “weight” \mathcal{W}_1 . The function \mathcal{W}_1 [and \mathcal{W}_2 from Eq.1.4] is given explicitly, e.g., in Ref. [3]. In the collinear limit, F_{LL}^h reduces to the well-known product of the collinear helicity distribution $g_1^q(x)$ and the collinear fragmentation function $D_1^{q \rightarrow h}(z)$. While there are no possible azimuthal moments at leading twist, cosine modulations are potentially present at twist-three level, i.e., suppressed by a single power of M/Q . Taking the Wandzura–Wilczek approximation (neglecting interaction-dependent terms, which depend on quark-gluon-quark correlators, and neglecting terms linear in quark masses) [6], the following expression remains:

$$F_{LL}^{h, \cos \phi} \propto \frac{M}{Q} \sum_q e_q^2 \left[g_{1L}^q(x, p_T^2) \otimes_{\mathcal{W}_2} D_1^{q \rightarrow h}(z, k_T^2) \right]. \quad (1.4)$$

This combination of distribution and fragmentation functions was studied, e.g., in Ref. [7], and is sometimes referred to as the “polarized Cahn effect”, which combines transverse momentum of longitudinally polarized partons inside the target nucleon with transverse momentum produced in the fragmentation process.

2. Results

It is the main goal of this work to present the kinematic dependences of hadron-tagged longitu-

dinal double-spin asymmetries as completely as possible with the available data. In comparison to the analysis of the HERMES unpolarized data presented in Ref. [8], the size of the data presented here did not allow for a complete five-dimensional kinematic unfolding of the data. Decisions were made about the best possible kinematic projections of these data, within the constraints of the theoretical framework described above and with the goal of providing the maximum possible access to physics of interest.

2.1 The semi-inclusive asymmetry binned in three dimensions

The hadron-tagged longitudinal double-spin asymmetry binned simultaneously in x , z , and $P_{h\perp}$ as measured by HERMES for hydrogen and deuterium targets are presented in Figs. 2. The asymmetry is binned in a grid with nine bins in x , three bins in $P_{h\perp}$, and three bins in z , and is plotted as a function of x for those ranges in z and $P_{h\perp}$. The binning was selected to populate the bins with statistics as uniformly as reasonable while maintaining a degree of kinematic uniformity across each bin. Within the precision of the measurements, the asymmetries display no obvious dependence on the hadron variables.

2.2 Azimuthal asymmetries

As described in the introduction, azimuthal moments of asymmetries are potentially sensitive to unique combinations of distribution and fragmentation functions, a number of which vanish when integrated over semi-inclusive kinematic parameters. The $P_{h\perp}$ projections of the $\cos\phi$ moments for charged pions for each target, as well as for charged kaons in case of a deuterium target are presented in Fig. 3. For each hadron and target combination, the asymmetry is divided into 10 ϕ bins and fit with an azimuthally periodic function in each of either $2x \times 5z$ -bins, $2x \times 5P_{h\perp}$ -bins, or $2z \times 5x$ -bins. The functional form used included constant, $\cos\phi$, and $\cos 2\phi$ terms. Each of these cosine moments is found to be consistent with zero. (A similar result was obtained for unidentified hadrons for deuteron data from the COMPASS experiment [11], [9].) The $P_{h\perp}$ projections of the $\cos\phi$ moments for charged pions for each target, as well as for charged kaons in case of a deuterium target are presented in Fig. 3. A vanishing $\cos 2\phi$ asymmetry as found here can be expected because in the one-photon-exchange approximation there is no $A_{LL}^{h,\cos 2\phi}$ contribution to the cross section [cf. Eq. 1.1] and thus a non-zero $A_{\parallel}^{h,\cos 2\phi}$ can arise in this approximation only through the very small transverse component of the target-spin vector in a configuration where the target is polarized along the beam direction [5].

2.3 The hadron charge-difference asymmetry

The hadron charge-difference asymmetry

$$A_1^{h^+ - h^-}(x) \equiv \frac{\left(\sigma_{1/2}^{h^+} - \sigma_{1/2}^{h^-}\right) - \left(\sigma_{3/2}^{h^+} - \sigma_{3/2}^{h^-}\right)}{\left(\sigma_{1/2}^{h^+} - \sigma_{1/2}^{h^-}\right) + \left(\sigma_{3/2}^{h^+} - \sigma_{3/2}^{h^-}\right)} \quad (2.1)$$

provides additional spin-structure information and is not trivially constructible from the simple semi-inclusive asymmetries. The difference asymmetries for pions from the hydrogen target and pions, kaons, and undifferentiated hadrons from the deuterium target are shown in Fig. 4, together with results from the COMPASS Collaboration for unidentified hadrons from a ${}^6\text{LiD}$ target [10].

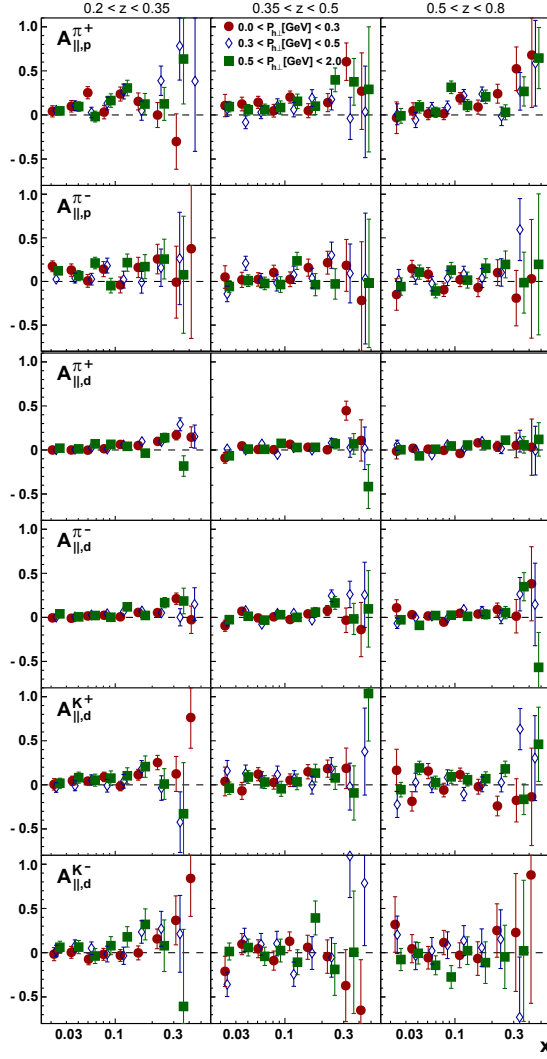


Figure 2: $A_{||,N}^h(x, z, P_{h\perp})$ as a function of x in three different z ranges and three different $P_{h\perp}$ ranges as labeled, with $N = p, d$ denoting the target nucleus and $h = \pi^\pm, K^\pm$ the final-state hadron detected. Data points for the second $P_{h\perp}$ slice are plotted at their average kinematics, while the ones for the remaining $P_{h\perp}$ slices are slightly shifted horizontally for better legibility. The inner error bars represent statistical uncertainties while the outer ones statistical and systematic uncertainties added in quadrature.

Under the assumption of leading-order (LO), leading-twist (LT) QCD, and charge-conjugation symmetry of the fragmentation functions, i.e.,

$$D_1^{q \rightarrow h^+} = D_1^{\bar{q} \rightarrow h^-}, \quad (2.2)$$

the difference asymmetry on the deuteron may be equated to a certain combination of parton distributions [12]:

$$A_{1,d}^{h^+ - h^-} \stackrel{\text{LO LT}}{=} \frac{g_1^{u_v} + g_1^{d_v}}{f_1^{u_v} + f_1^{d_v}}. \quad (2.3)$$

Here, $f_1^{q_v} \equiv f_1^q - f_1^{\bar{q}}$ ($g_1^{q_v} \equiv g_1^q - g_1^{\bar{q}}$) is the polarization-averaged (helicity) valence-quark distribution of the proton, and ‘‘LO LT’’ is a reminder of the assumptions mentioned previously. This

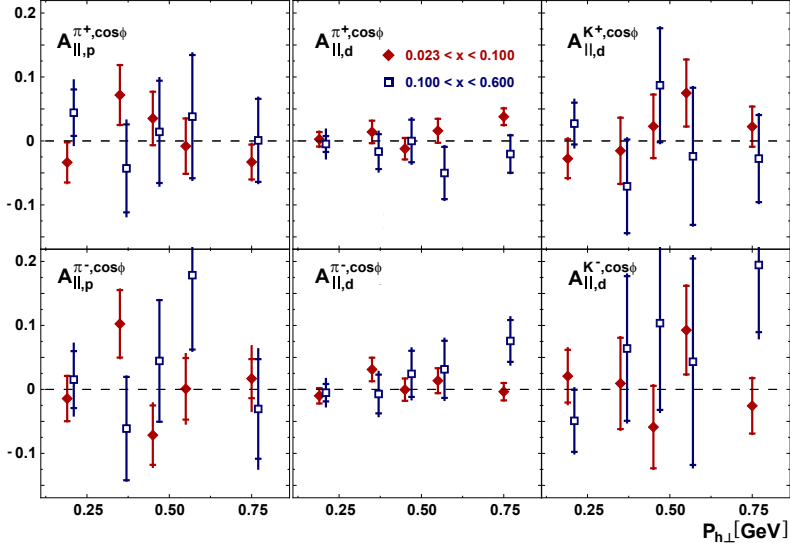


Figure 3: $A_{||}^{h, \cos \phi}(P_{h\perp})$ in two x ranges for charged pions (and kaons) from protons (deuterons) as labelled. The inner error bars represent statistical uncertainties while the outer ones statistical and systematic uncertainties added in quadrature. Data points for the first x slice are plotted at their average kinematics, while the ones for the second x slice are slightly shifted horizontally for better legibility.

is equivalent to assuming a well differentiated current and target region; a scenario in which the struck quark has no memory of the hadron variety to which it previously belonged.

By further assuming isospin symmetry in fragmentation, that is

$$D_1^{u \rightarrow \pi^+} = D_1^{d \rightarrow \pi^-}, \quad D_1^{u \rightarrow \pi^-} = D_1^{d \rightarrow \pi^+}, \quad (2.4)$$

a second valence-quark expression using charge-difference asymmetries from a hydrogen target is given by

$$A_{1,p}^{h^+ - h^-} \stackrel{\text{LOLT}}{=} \frac{4g_1^{u_v} - g_1^{d_v}}{4f_1^{u_v} - f_1^{d_v}}. \quad (2.5)$$

It follows that the charge-difference asymmetries should be independent of the hadron type, a feature consistent with the results shown in Fig. 4. Valence-quark helicity densities computed using Eqs. 2.3 and 2.5 are presented in Fig. 5 alongside the same quantities computed from the previous HERMES purity extraction [?]. The results are largely consistent using two methods that have very different and quite complementary model assumptions. Whereas the method presented here depends on leading-order and leading-twist assumptions to provide the clean factorization, which ensures that fragmentation can proceed without memory of the target configuration, the purity method depends on a fragmentation model subject to its own uncertainties related to the model tune and the believability of its phenomenologically motivated dynamics. The lack of dependence on hadron type of the charge-difference asymmetries and the consistency of the derived valence-quark helicity distributions with the results of the purity analysis suggest that there is no significant deviation from the factorization hypothesis.

3. Conclusion

Several longitudinal double-spin asymmetries in semi-inclusive deep-inelastic scattering have been presented. They extend the analysis of the previous HERMES publications to include also transverse-momentum dependence. Azimuthal moments, $A_{\parallel}^{h,\cos\phi}$, are found to be consistent with zero. The hadron charge-difference asymmetry $A_1^{h^+-h^-}(x)$ yields valence-quark helicity densities consistent with the result of the prior HERMES purity extraction. A common thread among these results is that within the available statistical precision the longitudinal sector shows no deviation from the leading-order, leading-twist assumption. In addition to this interpretation, these data are expected to provide an essentially model-independent constraint for theory and parameterization as they provide the first ever longitudinal double-spin semi-inclusive dataset binned in as many as three kinematic variables simultaneously. They point the way to future precision tests of models of nucleon structure that go beyond a collinear framework.

References

- [1] A. Airapetian et al. (HERMES collaboration), Phys. Rev., D71, 032004 (2005). hep-ex/0412027
- [2] P.J. Mulders and R.D. Tangermann, Nucl. Phys. B461, 197 (1996), hep-ph/9510301
- [3] A. Bacchetta, M. Diehl, K. Goeke, A. Metz, P.J. Mulders and M. Schlegel, JHEP 02, 093 (2007), hep-ph/0611265

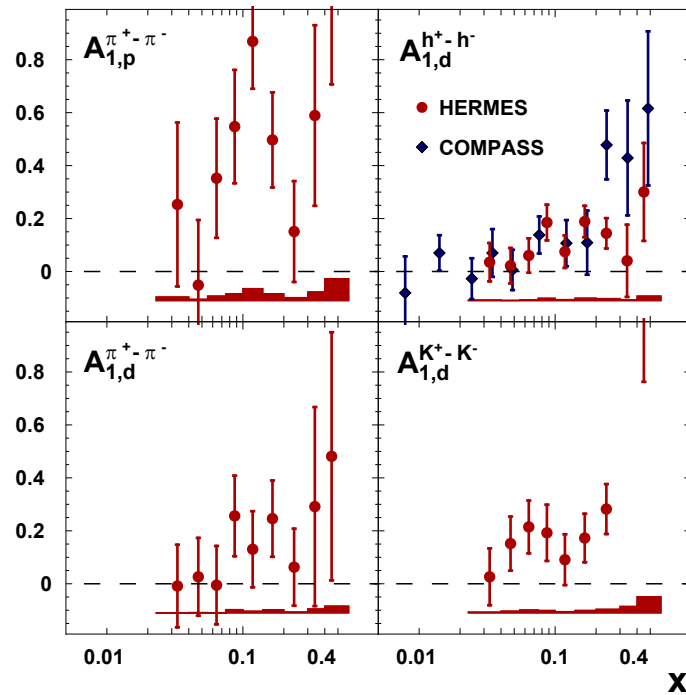


Figure 4: Hadron charge-difference asymmetries for pions from the hydrogen target and pions, kaons, and all hadrons from the deuterium target. Error bars represent statistical uncertainties. Systematic uncertainties are given as bands. Data from COMPASS [10] for undifferentiated hadrons using a ${}^6\text{LiD}$ target are also shown.

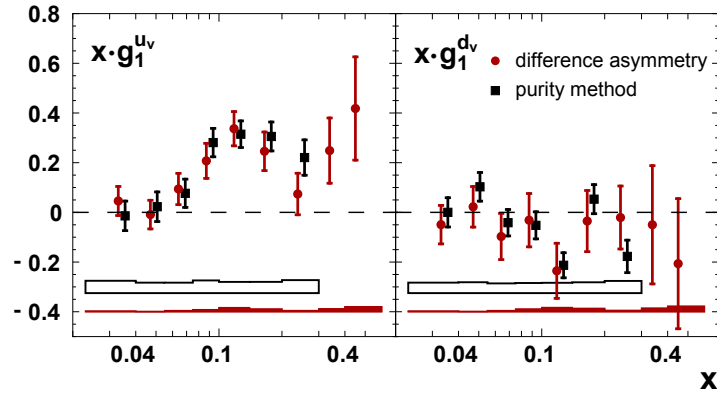


Figure 5: Helicity distributions for valence quarks computed using pion charge-difference asymmetries and Eqs. 2.3 and 2.5 compared with valence-quark densities (as indicated) computed from the HERMES purity extraction [1]. Error bars represent statistical uncertainties. Systematic uncertainties from the difference-asymmetry (purity) extraction are shown as filled (open) bands.

- [4] A. Bacchetta, U. D'Alesio, M. Diehl and C.A. Miller, Phys.Rev. D70, 117504 (2004), hep-ph/0410050
- [5] M. Diehl and S. Sapeta, Eur. Phys. J. C41, 515 (2005), hep-ph/0503023
- [6] S. Wandzura and F. Wilczek, Phys. Lett. B72, 195 (1977)
- [7] K.A. Oganessyan, P.J. Mulders and E. De Sanctis, Phys. Lett. B532, 87 (2002), arXiv:hep-ph/0201061 [hep-ph]
- [8] A. Airapetian et al. (HERMES Collaboration), Phys.Rev. D87, 012010 (2013), arXiv:1204.4161 [hep-ex]
- [9] C. Adolph et al. (COMPASS collaboration) (2016) arXiv:1609.06062 [hep-ex]
- [10] M. Alekseev et al. (COMPASS collaboration), Phys. Rev., B660, 458 (2008), arXiv:0707.4077 [hep-ex]
- [11] M. Alekseev et al. (COMPASS collaboration), Eur. Phys., J. C70, 39 (2010), arXiv:1007.1562 [hep-ex]
- [12] L.L. Frankfurt, M.I. Strikman, L. Mankiewicz, A. Schäfer, E. Rondio, A. Sandacz, and V. Papavassiliou, Phys.Lett., B230, 141 (1989)